Presented at the 25th European PV Solar Energy Conference and Exhibition, 6-10 September 2010, Valencia, Spain

INVESTIGATIONS ON INTERCONNECTION TECHNOLOGIES FOR CPV SYSTEMS

Maike Wiesenfarth, Stefan Thaller, Joachim Jaus, Fabian Eltermann, Michael Passig and Andreas W. Bett
Fraunhofer Institute for Solar Energy Systems ISE, Heidenhofstraße 2, 79110 Freiburg, Germany
phone: +49 761 4588 5470, fax: +49 761 4588 9250, maike.wiesenfarth@ise.fraunhofer.de

ABSTRACT: Long lifetime of concentrator photovoltaic systems strongly depends on the reliability of the interconnection technologies. In this paper the result of experiments to investigate the long term stability of a lead free $Sn_{95.5}Ag_4Cu_{0.5}$ solder alloy and two isotropic conductive adhesives are presented. Samples were subjected to accelerated aging consisting of high temperature storage at 150 °C and temperature cycles between -30 and 125 °C. The samples were characterised after various aging steps by x-ray imaging, scanning electron microscope and energy dispersive x-ray. The experiments showed a degradation of the soldered samples through the formation of cracks in the joint. Also a growth of brittle intermetallic phases was determined which can promote the generation of cracks. One of the tested adhesives shows a positive post curing and no degradation after aging. The second adhesive shows some cracks after the hard tests.
Keywords: Concentrator Cells, System, Degradation, Lifetime, Interconnection Technologies

1 INTRODUCTION

In concentrator photovoltaic modules, the management of thermal energy is essential. Most of the radiative energy from the sunlight that is not converted to electrical energy is transformed into thermal energy (heat). The heat needs to be conducted to a heat sink which is actively or passively cooled. Solder alloys or conductive adhesives are commonly used to attach the solar cell to the heat sink. The major requirements for the interconnection are high thermal and electrical conductivity as well as temperature resistance up to 120 °C. For reliable module operation, these properties must be maintained during the whole service life. This requires excellent longterm stability despite the thermal stress induced by the different thermal expansion coefficients of the components. The understanding of the degradation mechanisms like temperature effects and thermal stress is crucial for the design of concentrator modules. In this paper the influence of the mechanisms are investigated and determined through accelerated reliability tests. The objective of the experiments is to compare the performance of soldered and glued joints after accelerated aging and to evaluate the applicability for CPV modules.

2 APPROACH

For the accelerated reliability experiments, various test samples of solar cell assemblies, consisting of solar cells/diodes, conductive interconnection and heat sinks were produced. Soldered samples of the lead free alloy SAC ($Sn_{95.5}Ag_4Cu_{0.5}$) and two electrically and thermally isotropic conductive adhesives (ICA) from different manufacturers were tested. The test samples of solar cell assemblies were prepared with dummy solar cells (Ag back surface metallisation) soldered or glued to copper heat sinks (plated with Ni/Au). The soldered samples were produced in a reflow process. An overview of the samples and a sketch of the assembly can be seen in Figure 1.

samples	material
solder	$Sn_{95.5}Ag_4Cu_{0.5}$
adhesive 1	silver + epoxy
adhesive 2	silver + thermoplastic

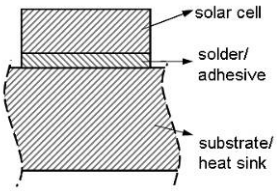

Figure 1: Table of the sample materials and sketch of the sample assembly.

The accelerated aging procedures used were high temperature storage (HTS) (1000 h at 150 °C) and temperature cycling (TC) (2000 temperature cycles between -30 and 125 °C). In addition, a combination of the tests with 500 h at 150 °C and almost 4000 temperature cycles was performed. The results of the latter are presented in this paper as this is the longest testing period. Regarding the test conditions, higher temperatures and longer testing duration were chosen than those of the industry testing standard of the international electrotechnical commission IEC 62108. The reason is that operating temperatures of the solar cell are expected to reach 90 °C [1] in passively cooled systems with lenses and an aperture of 40x40 mm². This temperature will be even higher for systems with increased lens sizes or reduced heat sink sizes. In actively cooled systems the cell temperature would necessarily be higher than the cooling fluid temperature. The cell temperature can be kept below 60 °C for cooling water at ambient temperature [2]. However, to provide hot process water or to increase the fluid/air heat exchange, it is desirable to increase the cooling fluid temperature to 85 °C or higher. Given a thermal resistance of 0.4 (K*cm²)/W and a heat flux of 85 W/cm², the solar cell temperature is almost 120 °C.

To characterise the joint of the samples, non-destructive and destructive characterisation methods (x-ray images and shear tests) were chosen. Furthermore, metallographic cross sections were examined by optical microscope, scanning electron microscope (SEM) and energy dispersive x-ray (EDX). In total more than 340 samples were prepared and characterised.

3 EXPERIMENTAL RESULTS

3.1 Measurement of the maximum shear force

The adhesion of the diode to the substrate was determined by shear tests. The shear tests were carried out after each aging step for at least 5 samples. The shear force was measured when the diode sheared from the substrate. In Figure 1 the average shear force is shown for samples when the complete diode is detached from the substrate. The average shear force and the standard deviation for each aging step are given.

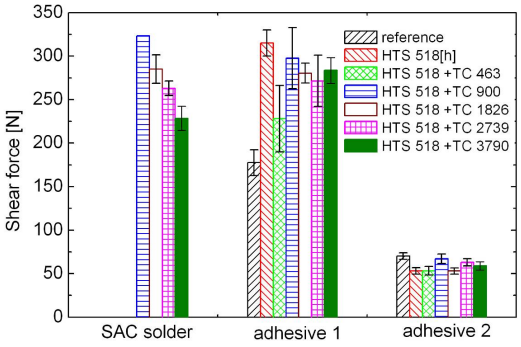

Figure 2: Average shear forces for soldered and glued samples after different aging steps.

After 518 h of temperature annealing and 900 temperature cycles, the average shear force for soldered samples was the highest with 322 N. A degradation of the solder bond is determined due to decreasing shear force with successive aging steps. After 518 h of temperature annealing and 3790 temperature cycles, the average shear force is 229 N.

The glued samples do not show this decrease of the shear force with duration of the aging. On the contrary, the shear force even increases after the first aging steps. This indicates a post curing of the polymer in the adhesive.

The shear tests showed that adhesive 1 has the highest level of shear forces, varying between 178 N and 315 N. After examining the fracture pattern the shear tests also showed that for the reference samples of adhesive 1, the substrate and adhesive layer delaminated without residues (adhesion fracture). After temperature storage, the shear strength increases and cohesive failures are observed. The average shear forces of adhesive 2 are between 53 N and 70 N. No significant change after aging can be observed.

The samples in which the diode broke during the tests are not included in the diagram. The reason is that these experiments do not give the shear force of the bonding layer, but rather the shear force of the diode as the strength of the semiconductor material is lower than that of the bonding layer. In Table I an overview of the samples with broken diodes and the number of shear tested samples is given. All diodes broke for soldered samples of the reference, first and second ageing step and that is why there bars in the diagram of Figure 1 are shown. During tests of samples of the third, fourth and fifth aging step, various diodes broke as well. Some diodes of adhesive 1 samples broke of the first, second, third, fifth and sixth aging steps. No diodes broke during shear tests of adhesive 2 samples. This means by comparing the fracturing modes for the different materials, it can be concluded that the maximum shear force for this assembly with a silicon diode of size 3.5 x 2.5 mm² is between 300 and 350 N.

Table I: Quantity of shear tested samples and quantity where the diode broke for soldered and glued samples during the different aging steps:

Batch	**Solder**		**Adhesive 1**		**Adhesive 2**	
Fracture pattern	**samples**	**diode broke**	**samples**	**diode broke**	**samples**	**diode broke**
Reference	5	5	5	0	5	0
HTS 518	6	6	6	1	6	0
HTS 518/TC463	6	6	6	3	6	0
HTS 518/TC900	7	6	6	1	6	0
HTS 518/TC1826	6	3	6	0	6	0
HTS 518/TC2739	6	1	6	1	6	0
HTS 518/TC3790	5	0	6	1	6	0

3.2 Examination of soldered interconnection layers

Figure 3 shows the result of an x-ray examination of one soldered sample before accelerated aging (left) and the same sample after 518 h HTS and 3790 temperature cycles (right picture). There are areas without solder, e.g. voids (trapped air). The voids that were already formed during the manufacturing process do not grow due to degradation as they have the same size before and after the aging test. The image on the right clearly shows degradation of the solder layer, as cracks and other voids formed during aging.

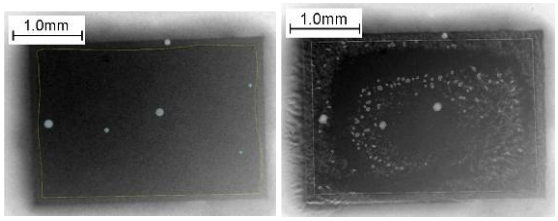

Figure 3: X-ray image of a soldered sample before accelerated aging (left) and after 518 h temperature annealing (150 °C) and 3790 temperature cycles (-30 °C and 125 °C).

The intermetallic compounds (IMC) in the solder layer change due to thermal diffusion processes. The material compositions were determined by EDX-examination of metallographic preparations. SEM images of microsections before and after accelerated aging are shown in Figure 4 including the results of EDX. The solder alloy $Sn_{95.5}Ag_4Cu_{0.5}$ mainly consists of tin which is determined to be the main part in the interconnection. The EDX examination reveals that during the soldering process, the solder alloy and the silver surface of the diode build an intermetallic phase of Ag_3Sn. On a nickel barrier layer, between solder and substrate, an intermetallic phase IMC 1 of $(Ni,Cu)_3Sn_4$ is formed. These intermetallic phases are essential for a good bonding [3]. During the reflow process the gold on the surface of the substrate diffuses quickly into the soldering layer. Within the joint of the sample a gold-tin ($AuSn_4$) compound was determined. The immediate dissolution is also described in Mattila *et al* [3]. In the soldering layer, intermetallic phases of silver and tin (Ag_3Sn) or copper and tin are also accumulated. As the copper content is not distributed homogeneously, different Cu-Sn compounds are formed [5]. The Ag_3Sn

and Cu-Sn IMCs are needle or rod-shaped and distributed homogenously in the bulk of the joint in the top picture of Figure 4. This is a typical microstructure for an SAC solder as it was published for example in Ma *et al* [4].

By comparing the SEM images of Figure 4, it can be seen that the intermetallic phases grow with the aging process. The thickness of the intermetallic phase IMC 1 $(Ni,Cu)_3Sn_4$ between the solder and the substrate especially increases with aging. Furthermore, in the bottom picture the second intermetallic phase IMC 2 becomes visible (bright area above IMC 1). This is well known from literature and usually is a phase of $(Ni,Cu)_6Sn_5$ [3]. In this experiment the material composition was not determined by the EDX examination because the grain size of IMC 2 was below the resolution.

During accelerated aging, the IMCs within the bulk of the interconnection layer accumulate and grow. The needle shape gets round and the IMCs become plates. Intermetallic compounds of $(Ni,Cu)_3Sn_4$, $(Ni,Cu)_5Sn_6$, $(Au,Ni)Sn_4$ and Ag_3Sn are determined. The growth of the IMCs is due to thermal diffusion of copper and nickel from the substrate.

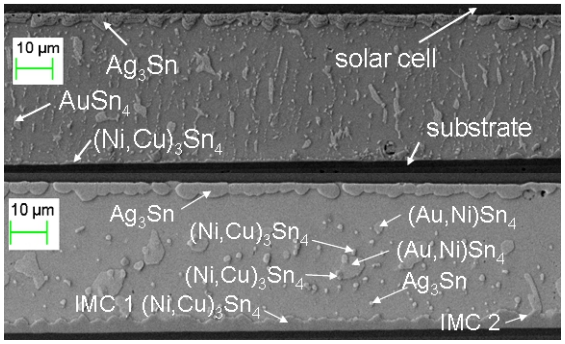

Figure 4: SEM-image of a soldered sample before aging (top) and after 518 h HTS and 3790 temperature cycles (bottom). Determined by the EDX examination, the material compositions of the phases in the solder layer are given.

After HTS and TC, cracks could be observed which propagate through the solder joint. The cracks often start at the edge between diode and solder alloy. A crack of a soldered sample after temperature annealing and 3790 temperature cycles is shown in Figure 5. The crack goes through the tin-silver-solder layer and is stopped or redirected by IMCs (Figure 5 bottom right). The crack runs between the IMCs and the diode.

According to Leng et al. [6] the intermetallic phase of copper and tin is brittle. This can be observed in the left picture of Figure 5 (bottom) which shows a typical start of a crack at the interface between IMC and tin main-phase. This means that a growth of the IMCs can reduce the strength of the joint especially at the IMC between solder and substrate or diode respectively. As it was observed that cracks are redirected by the IMCs it can be concluded that a homogeneous distribution of many small sized IMCs is preferred to few large IMCs in the bonding layer.

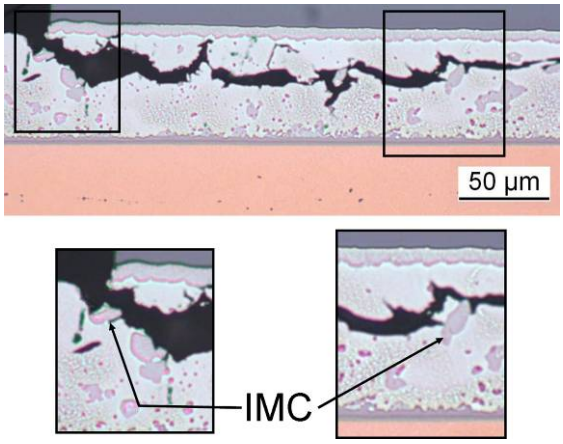

Figure 5: Image of a section of a metallographic specimen of a soldered sample after 518 h temperature annealing and 3790 temperature cycles. A crack is shown which begins at the edge of chip and solder and leads into the bonding layer close to the chip surface (top). Enlarged view of the section where the crack starts and is redirected by the IMC and runs above the IMCs (bottom).

3.3 Examination of glued interconnection layers

Figure 6 shows the result of an x-ray examination of a typical glued sample with adhesive 2 after manufacturing (left) and the same sample after 518 h of temperature annealing and 3790 temperature cycles (right picture). There is no visible degradation, as was observed for both tested types of adhesive.

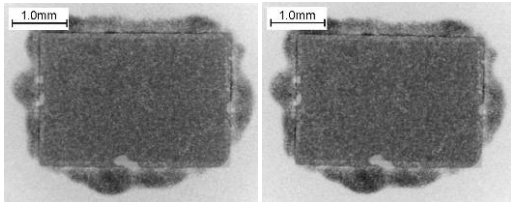

Figure 6: X-ray image of a glued sample (adhesive 2) before accelerated aging (left) and after 518 h HTS (150 °C) and 3790 temperature cycles (-30 °C and 125 °C).

Glued samples were examined by SEM. Samples are shown in Figure 7 for adhesive 1 (top) and adhesive 2 (bottom). The adhesives are thermally and electrically conductive. The adhesion is provided by an epoxy (adhesive 1) and a thermoplastic resin (adhesive 2). The thermal conduction of ICAs is improved by silver particles in the compound [7]. The black areas in the SEM images in Figure 7 are epoxy or thermoplastic resin, the silver particles are grey. The silver content of adhesive 1 in the top picture is lower than that of adhesive 2.

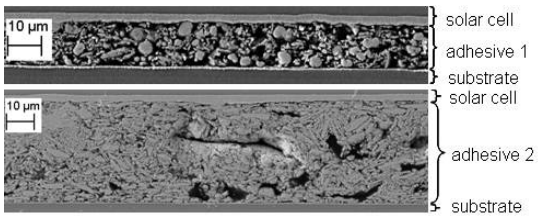

Figure 7: SEM image of a sample with adhesive 1 (top) and adhesive 2 (bottom).

The layer thickness varies among the samples. Adhesive 1 has a layer thickness of about 10 µm, adhesive 2 has a thickness of about 40 µm. The layer thickness is a result of production process parameters as well as paste parameters. For the specific assembly, standard production parameters and not optimised process parameters have been used.

The shape of the silver particles is also different across the adhesive samples. In adhesive 1 the particles mainly have a round shape, whereas the particles in adhesive 2 basically have a flat long shape. The areas of the particles` cross sections are similar. This will influence the thermal resistance of the adhesive, as the thermal energy is conducted by the silver particles and is improved by touching particles. A low thermal resistance gives a low temperature difference between the solar cell and substrate.

The cross-section of adhesive 2 shows clusters of thermoplastic resin of 5 to 8 µm in diameter (black areas in Figure 7). One corrective approach to reduce the quantity of the clusters could be to improve the mixing procedure of the adhesive before processing.

In Figure 8 the cross-section of a sample of adhesive 1 is shown after high temperature storage and temperature cycling. By comparing it to the top picture of Figure 7, no differences could be observed. Hence for adhesive 1, no degradation can be determined when investigating the metallographic specimens after the aging tests.

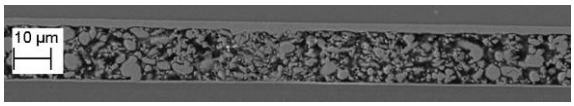

Figure 8: SEM-image of a section of a metallographic specimen of adhesive 1 after 518 h HTS and 3790 temperature cycles.

The microsections of adhesive 2 do not show a consistent aging effect. Samples aged by temperature annealing (1000 h) do not show degradation. The shear test showed no decrease of the maximum shear force.

In Figure 9 an image of a microsection aged by HTS and 1820 h temperature cycles is shown. A horizontal crack through the complete section can be observed. In this aging batch, two crack mechanisms occur. One crack propagates through the chip itself and the adhesive delaminates from the back surface of the chip. Other cracks propagate through the adhesion layer.

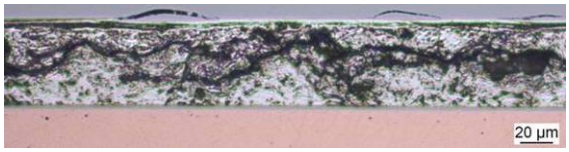

Figure 9: Microscope-image of a centre section of a metallographic specimen of adhesive 2 after 518 h HTS and 1820 temperature cycles. There are visible cracks in the adhesive layer.

In contrast, no cracks are visible in the centre section of Figure 10 (top), although the sample was aged by 1970 additional temperature cycles. In Figure 10 (bottom) the microsection shows delamination at the edge of the diode edges. There is also a crack starting from the void at the edge and growing into the direction of the centre of the diode. As the characterisation method is destructive, the same sample cannot be analysed before and after the aging test. The cracks could not be determined by the x-ray images.

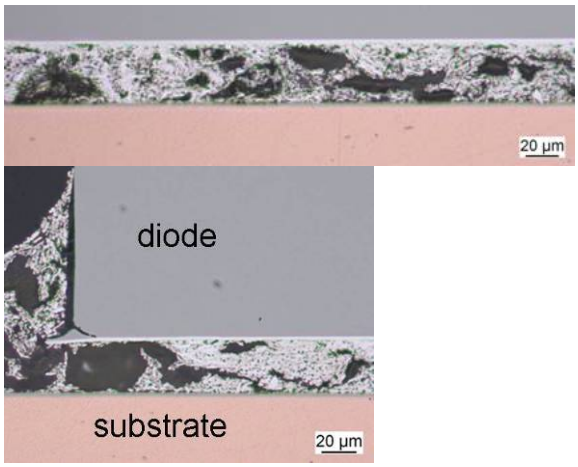

Figure 10: Microscope-image of a centre and an edge section of a metallographic specimen of adhesive 2 after 518 h temperature annealing and 3790 temperature cycles. No cracks can be seen in the centre of the interconnection (top). A crack is identified at the edge of the sample.

Comparing the metallographic preparations of adhesive 1 and adhesive 2, it can be concluded that adhesive 1 does not show a decrease in reliability whereas the reliability of adhesive 2 needs to be investigated further. Comparing the thermal resistance, adhesive 2 has a lower thermal resistance than adhesive 1.

4 DISCUSSION AND SUMMARY

Comparing bonds of solder and adhesive, the difference is that solders build intermetallic phases by diffusion processes. The adhesion of glues takes place at the interface between the component and the bonding material. This causes a contact resistance (thermal and electrical) for conductive adhesives at the boundary layer [8]. The shear strength is defined by this interface and usually is lower than for solders. Because of the resin, the adhesives are more flexible than soldered connections. This means they can allow for some thermo-mechanical stress. Hence adhesives are less sensitive to thermal cycling. In the experiments presented in this paper the temperature cycling did not degrade samples of adhesive 1. For samples of adhesive 2 thin cracks were determined after 500 h HTS and 4000 temperature cycles. The soldered samples show changes in the material composition due to thermal diffusion processes. The intermetallic phases grow with HTS and due to their brittleness cracks tend to be formed when temperature cycled. In CPV applications, a combination of stress due to high temperatures and temperature cycles is very common.

In the experiments the shear test showed that the initial shear strength varies between the test batches of solder and adhesives. The soldered samples have the highest maximum shear force (before fracturing) of

322 N after 518 h of HTS and 900 TC. With 178 N, the shear strength of the reference samples of adhesive 1 is almost half and with 70 N the shear force of adhesive 2 samples more than four times lower than the shear force of the soldered samples. The behaviour changes with the aging. After 518 h HTS and 3790 temperature cycles, the average shear force of the soldered sample is 229 N. The shear force of adhesive 1 increases to 284 N and the shear force of adhesive 2 decreases slightly to 59 N. The degradation of the solder bond with successive aging steps was also determined by the x-ray examination. EDX examination shows a change of the intermetallic phases. The increase of the shear strength of adhesive 1 indicates a post curing of the adhesive. The shear strength of adhesive 1 is higher than for adhesive 2 which can be due to the higher epoxy content in adhesive 1 as observed in the metallographic preparations. On the other hand, with the higher content of silver flakes, the thermal resistance of adhesive 2 is lower than for adhesive 1. This shows that the selection of suitable bonding material, production process and manufacturer is extremely important.

Compared to the test sequences of IEC 62108, the temperature level and test duration is enhanced. Even so, during the experiments neither the solder alloy nor adhesive showed a complete failure.

5 CONCLUSION AND OUTLOOK

For CPV applications the electrical and thermal properties of the connection between the solar cell and the heat sink are essential. The accelerated aging revealed differences between the solder alloys and conductive adhesive that were used. The solder alloy shows degradation after 500 h HTS and almost 4000 temperature cycles in accelerated aging tests. Adhesive 1 does not show degradation when examined by x-ray or metallographic preparations. Some samples of adhesive 2 show cracks in the metallographic preparation but the degradation is not determined in the shear tests. Still after the experiments the shear forces of the soldered samples is higher than for adhesive 2.

The properties of solders and adhesives differ in thermal resistance. The solder alloy has a better thermal conductivity than the mixture of resin and silver flakes. In addition, for adhesives a thermal resistance at the interface between the components and glue is increased. In future experiments the effect of cracks and delamination on the thermal resistance, hence on the temperature of the solar cell, a will be determined. In addition, the electrical contact resistance after reliability testing will be investigated.

7 ACKNOWLEDGEMENT

The authors would like to thank A. Paproth from TU Dresden for the metallographic preparations. This work has been partly supported by the Federal Ministry for the Environment, Nature Conservation and Nuclear Safety (BMU) under the KoMGen project, contract number 0327567A. The authors are responsible for the content of this paper.

7 REFERENCES

[1] J. Jaus, R. Hue, M. Wiesenfarth, G. Peharz, A.W. Bett, “Thermal Management in a Passively Cooled Concentrator Photovoltaic Module”, 23rd European Photovoltaic Solar Energy Conference and Exhibition, 1-5 September 2008, Valencia, Spain, pp. 832-836.

[2] P.J. Verlinden, A. Lewandowski, H. Kendall, S. Carter, K. Cheah, I. Varfolomeev, D. Watts, M. Volk, I. Thomas, P. Wakeman, A. Neumann, P. Gizinski, D. Modra, D. Turner, J.B. Lasich, “Update on two-year performance of 120 kWp concentrator PV systems using multi-junction III-V solar cells and parabolic dish reflective optics”, 33rd Photovoltaic Specialists Conference, 2008, San Diego, USA.

[3] T. T. Mattila, T. T. Laurila, J. K. Kivilahti, “Reliability of high-density lead-free interconnections”, Preprinted from E. Suhir, C. P. Wong, and Y. C. Lee, “Micro- and Opto-Electronic Materials and Structures: Physics, Mechanics, Design, Reliability, Packaging”, Springer Science+Business Media, 2005, pp. 313 – 349.

[4] H. Ma, J. C. Suhling, Y. Zhang, P. Lall, M.J. Bozack, “The influence of elevated temperature aging on reliability of lead free solder joints”, 57th IEEE Electronic Components and Technology Conference, 2007, Reno, USA, pp. 653-666.

[5] A. Ourdjini, M.A. Azmah Hanim, S.F. Joyce Koh, I. Siliti Aisha, K.S. Tan, Y.T. Chin, “Effect of solder volume on interfacial reactions between eutectic Sn-Pb ans Sn-Ag-Cu solders and Ni(P)-Au surface finish”, IEEE International Electronic Manufacturing Technology, 2006, Putrajaya, Malaysia, pp. 437-442.

[6] E.P. Leng, M. Ding, A.T. Ling, N. Amin, I. Ahmad, M.Y. Lee, A.S.M.A. Haseeb, “A study of SnAgNiCo vs Sn3.8Ag0.7Cu C5 lead free solder alloy on mechanical strength of BGA solder joint”, 10th Electronics Packaging Technology Conference, 2008, Singapore, Singapore, pp. 588-594.

[7] J. Lee, C. S. Cho, J. E. Morris, “Electrical and reliability properties of isotropic conductive adhesives on immersion silver printed-circuit boards”, Microsystem Technologies Volume 15, Number 1, Springer Verlag, 2009, pp. 145-149.

[8] J.C. Jagdt, “Reliability of electrically conductive adhesive joints for surface mount applications: A summary of the state of the art”, IEEE Transactions on Components, Packaging, and Manufacturing Technology, Part A, volume 2, 1998, pp. 215-225.